

Copyright Warning & Restrictions

The copyright law of the United States (Title 17, United States Code) governs the making of photocopies or other reproductions of copyrighted material.

Under certain conditions specified in the law, libraries and archives are authorized to furnish a photocopy or other reproduction. One of these specified conditions is that the photocopy or reproduction is not to be “used for any purpose other than private study, scholarship, or research.” If a user makes a request for, or later uses, a photocopy or reproduction for purposes in excess of “fair use” that user may be liable for copyright infringement,

This institution reserves the right to refuse to accept a copying order if, in its judgment, fulfillment of the order would involve violation of copyright law.

Please Note: The author retains the copyright while the New Jersey Institute of Technology reserves the right to distribute this thesis or dissertation

Printing note: If you do not wish to print this page, then select “Pages from: first page # to: last page #” on the print dialog screen

The Van Houten library has removed some of the personal information and all signatures from the approval page and biographical sketches of theses and dissertations in order to protect the identity of NJIT graduates and faculty.

ABSTRACT

SIMULATION OF POLYMER SOLAR CELL CHARACTERISTICS BY AMPS-1D

**By
Lu Zhang**

Simulation of polymer solar cell characteristics is presented in this study. The solar cells are made of materials such as the following: Poly (3-hexylthiophene): [6, 6]-phenyl C₆₁-butyric acid methylester (P3HT: PCBM) and poly[2,1,3-benzothiadiazole-4,7-diyl[4,4-bis(2-ethylhexyl)-4H-cyclopenta[2,1-b:3,4-b']dithiophene-2,6-diyl]]: [6, 6]-phenyl C₆₁-butyric acid methylester (PCPDTBT: PCBM) are used as active layer materials. Analysis of Microelectronic and Photonic Structures One Dimension (AMPS-1D) is a computer simulation tool for solar cell device characteristics. The first part of this study focuses on the performance and comparison of current-voltage (I-V) simulations of indium oxide (In₂O₃) and tin oxide (SnO₂) (ITO) and poly (3,4-ethylenedioxythiophene): poly (styrenesulfonate) (PEDOT: PSS) as transport layer. The other comparison is between single polymeric solar cell and tandem polymeric solar cells by current-voltage (I-V) simulations. Photovoltaic effect permits the conversion of sunlight to electrical energy by excitons. Excitons travel from highest unoccupied molecular orbital (HOMO) level of conjugated polymer material to lowest unoccupied molecular orbital (LUMO) level of fullerene material. Exciton is regarded as a bound state of electron and hole.

**SIMULATION OF POLYMER SOLAR CELL CHARACTERISTICS
BY AMPS-1D**

**by
Lu Zhang**

**A Thesis
Submitted to the Faculty of
New Jersey Institute of Technology
in Partial Fulfillment of the Requirements for the Degree of
Master of Science in Materials Science and Engineering
Interdisciplinary Program in Materials Science and Engineering**

May 2012

Blank Page

APPROVAL PAGE

**SIMULATION OF POLYMER SOLAR CELL CHARACTERISTICS
BY AMPS-1D**

Lu Zhang

Professor N. M. Ravindra, Thesis Advisor
Professor of Physics, NJIT

Date

Dr. Michael Jaffe, Committee Member
Research Professor of Biomedical Engineering, NJIT

Date

Professor Tao Zhou, Committee Member
Associate Professor of Physics, NJIT

Date

BIOGRAPHICAL SKETCH

Author: Lu Zhang
Degree: Master of Science & Engineering
Date: May 2012

Undergraduate and Graduate Education:

- Master of Materials Science & Engineering,
New Jersey Institute of Technology, Newark, NJ, 2012
- Bachelor of Polymer Materials Science & Engineering,
Beijing University of Chemical Technology, Beijing, P. R. China, 2010

Major: Materials Science & Engineering

ACKNOWLEDGEMENTS

I would like to thank Professor Nuggehalli M. Ravindra, my master's thesis advisor for his constant advice, help and support. He is very kind of many ways. I would like to thank Drs. Michael Jaffe and Tao Zhou for their participation as members of my thesis committee. I thank Professor Marino Xanthos and Ms. Gonzalez-Lenahan who helped me with the language and grammar of my thesis. I would like to express my thanks to Zimeng Chen, Zhitao Wang and Zhaoqian Su who helped me with AMPS-1D. Finally, my most special thanks should be given to the Lord and to my parents who have been with me throughout my life.

TABLE OF CONTENTS

Chapter		Page
1	INTRODUCTION.....	1
	1.1 Background of Solar Cells.....	1
2	RESEARCH BACKGROUND.....	3
	2.1 Principle of Organic Photovoltaics.....	3
	2.1.1 Energy Transfer and Migration.....	3
	2.1.2 OPV Characterization.....	4
	2.1.3 Molecular Orbital Structures.....	6
	2.1.4 Conjugated Polymers' Chemical Structures.....	7
	2.2 Device Architecture.....	8
	2.2.1 Typical Device Architecture.....	8
	2.3 Tandem Polymeric Solar Cells.....	10
	2.3.1 The Need for Tandem Polymeric Solar Cells.....	10
	2.3.2 Fabrication of Tandem Polymeric Solar Cells.....	11
3	RESEARCH OBJECTIVE.....	14
4	EXPERIMENTAL DETAILS.....	15
	4.1 AMPS-1D.....	15
	4.2 Molecular Structures of Materials of Polymeric Solar Cells....	16
	4.3 Experimental Parameters and Design.....	17
	4.3.1 Parameters of Polymeric Solar Cell Materials.....	17
	4.3.2 Design of Comparable Experiments.....	22

TABLE OF CONTENTS
(Continued)

Chapter		Page
5	RESULTS, DISCUSSION AND CONCLUSIONS.....	25
	REFERENCES.....	30

LIST OF TABLES

Table		Page
4.1	General Experimental Data.....	17
4.2	PEDOT General Layer Data.....	18
4.3	PCBM General Layer Data.....	18
4.4	P3HT General Layer Data.....	19
4.5	PCPDTBT General Layer Data.....	19
4.6	ITO General Layer Data.....	19
4.7	PEDOT Band Tail Data.....	20
4.8	P3HT Band Tail Data.....	20
4.9	Thickness of Polymeric Solar Cell Layers.....	22
4.10	Thickness of Polymeric Solar Cell Layers.....	22
5.1	Characteristics of PEDOT Transport Layer Polymeric Solar Cells and ITO Transport Layer Polymeric Solar Cells	24
5.2	Characteristics of Single Polymeric Solar Cells and Tandem Polymeric Solar Cells.....	25
5.3	Generation Positions of Single and Tandem Polymeric Solar Cells.....	26

LIST OF FIGURES

Figure		Page
2.1	Plot of $\log(k_{ET})$ versus distance r for both Dexter (solid line) and Förster (dotted line) energy transfer mechanisms.....	4
2.2	Current-Voltage response of photovoltaic device under illumination....	5
2.3	Schematic illustration of the photoelectric conversion mechanism.....	6
2.4	A schematic of the hybridization and bonding in chemical structure.....	7
2.5	Chemical structure of conjugated polymers used in OPVs.....	8
2.6	Polymeric solar cell device structure.....	9
2.7	Typical tandem polymeric solar cell device.....	10
2.8	Thermo-treatment process.....	12
4.1	AMPS-1D main window.....	15
4.2	Molecular structures: PCBM, P3HT, PEDOT: PSS, PCPDTBT.....	17
4.3	Device structures of organic solar cells.....	22
4.4	Device structures of single polymeric solar cells and tandem polymeric solar cells.....	23
5.1	I-V curves: PEDOT transport layer polymeric solar cell versus ITO transport layer polymeric solar cell	24
5.2	I-V curves: Single polymeric solar cells and tandem polymeric solar cells.....	25

LIST OF ABBREVIATIONS

P3HT	Poly (3-hexylthiophene)
PCBM	[6, 6]-phenyl C ₆₁ -butyric acid methylester
PCPDTBT	Poly[2,1,3-benzothiadiazole-4,7-diyl[4,4-bis(2-ethylhexyl)-4H-cyclopenta[2,1-b:3,4-b']dithiophene-2,6-diyl]]
ITO	Indium oxide and tin oxide
PEDOT: PSS	Poly (3,4-ethylenedioxythiophene): poly (styrenesulfonate)
PPV	Poly (phenylene vinylene)
PT	Polythiophenes
PPE	Polyphenyl ethers
PPP	Poly (p-phenylene)
PFO	Polyfluorene
P3MHOCT	Poly (3-(2-methylhexyloxycarbonyl) dithiophene)
P3CT	Poly (3-chlorothiophene)
PT	Poly chlorothiophene

CHAPTER 1

INTRODUCTION

1.1 Background of Solar Cells

Photosynthesis is a biological process. The most common form is chlorophyll-type pigment which can capture the sun's energy and convert sunlight into biochemical energy needed for the plant life by a series of steps. Manmade Solar Cell is a device which can convert the energy of sunlight into electrical energy directly by a photovoltaic process. The first generation solar cell is a silicon solar cell that was invented by Russell Ohl in 1941 [1], but the energy conversion efficiency was less than one percent. Satellite Vanguard developed by Pentagon is the first practical application of silicon solar cells in 1955 [2]. Satellite Vanguard had silicon solar cells for its power requirements. The cost of space solar cells is in the millions of dollars, which kept it far from wide applications [3]. In 1968, Elliot Berman decided to quit his industrial chemist job and made efforts to lower the cost of silicon solar cells from \$200 per watt down to \$20 per watt.

Several kinds of materials are utilized to fabricate solar cells. These include the following: polycrystalline silicon, amorphous silicon, high-efficiency silicon, gallium arsenide and related III-V materials and thin-film materials including II-VI semiconductors. Thin film solar cell is the second generation solar cell, which has significant advantages of low cost, flexibility and easy fabrication process. GaAs has an ideal band gap of 1.42eV, and the energy conversion efficiency of GaAs cells can reach as high as 32%. Unfortunately, GaAs thin film solar cells also cost as high as million dollars. Until now, the first generation solar cell represents 86% of the solar cell market. At the end of 20th century, many advanced concepts were utilized to improve power

conversion efficiency. Multiple junction cells, concentrator cells, nanotechnology-specifically quantum dots and a process of low-temperature substrate were all used in thin film solar cell research. Even so there are still many challenges addressed by a variety of technologies. Available area, efficiency, reliability, light weight, easy process and, particularly, power at optimal cost are the specific issues that need to be addressed to make solar cells practical and viable from a commercial stand point. Taking them into account, organic photovoltaic devices can provide solutions in applications that: need low price; are used in recreational products and require environmental durability.

CHAPTER 2

RESEARCH BACKGROUND

2.1 Principles of Organic Photovoltaics

2.1.1 Energy Transfer and Migration

There are two non-radiative energy transfer mechanisms:

i. Förster: It is a type of through-space or dipole-dipole energy transfer, and involves a long-range coupling of donor dipole and acceptor dipole. The resonance between donor and acceptor dipole moment is facilitated by the presence of intervening solvent dipoles [4]. The energy transfer rate (k_{ET}) is described by the following equation:

$$k_{ET} = k * \frac{k_D^0 * \kappa^2}{R_{DA}^6} * J \quad (2.1)$$

k is a constant value (solvent index of refraction concentration).

κ^2 is related to interaction between the oscillating donor dipole and acceptor dipole.

k_D^0 is a pure radiative rate of donor.

J is the spectral overlap integral.

R_{DA} is the distance between donor and acceptor.

ii. Dexter: It is known as through-bond energy transfer and takes place through a double electron exchange mechanism within molecular orbitals of donor and acceptor [4].

The Dexter energy transfer rate k_{ET} is as follows:

$$k_{ET} = KJ * e^{\left(\frac{-2R_{DA}}{L}\right)} \quad (2.2)$$

L is the Van Der Waals radii of donor and acceptor.

K is related to the specific orbital interactions.

R_{DA} is the distance between donor (D) and acceptor (A).

The relationship between Dexter energy transfer mechanism and Förster energy transfer mechanism is described by Figure 2.1:

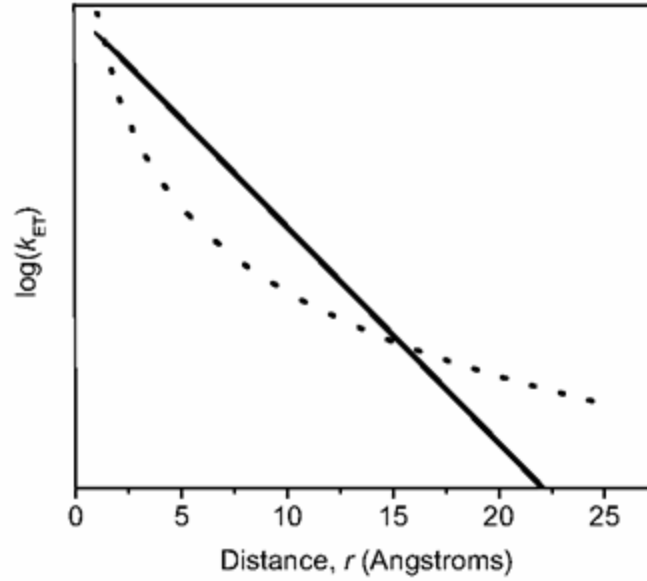


Figure 2.1 Plot of $\log(k_{ET})$ versus distance r for both Dexter (solid line) and Förster (dotted line) energy transfer mechanisms [4].

2.1.2 Solar Cell Characterization

Characteristics of solar cells are described by the following terms: short-circuit current (J_{SC}), open-circuit voltage (V_{OC}), fill factor (ff), maximum power (P_m), incident optical power (P_o) and power conversion efficiency (η_e).

$$ff = P_m / I_{SC} V_{OC} = I_m V_m / I_{SC} V_{OC} \quad (2.3)$$

$$\eta_e = I_m V_m / P_o = ff \times I_{SC} V_{OC} / P_o \quad (2.4)$$

The short-circuit current depends on photon absorption and internal conversion efficiency. By increasing the device thickness, the quantity of absorbed photons can be increased. Due to low charge mobility, the number of recombination charges in larger thickness will increase. Consequently, the fill factor will decrease due to the recombination loss.

In Figure 2.2, the fill factor can be represented by the ratio of the dark shaded part to the lightly shaded part of the curves.

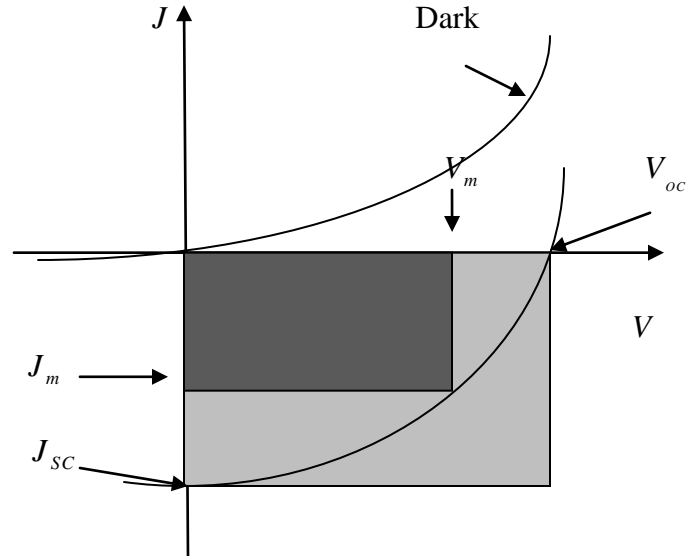


Figure 2.2 Current-Voltage response of photovoltaic device under illumination.

The incident photon conversion efficiency (external quantum efficiency), EQE is given by the number of electrons generated per incident photon:

$$EQE = \frac{n_e}{n_{ph}} = \frac{I_{sc}}{P_o} \frac{hc}{\lambda e} \quad (2.5)$$

In theory, the power efficiency of a solar cell can be calculated by integrating the EQE over the solar spectrum and multiplying by the monochromatic power efficiency [5].

The working principle of organic solar cells is that excitons are excited in organic materials, and the exciton, which is a bound electron-hole (positive charge carrier) pair, needs to dissociate into free charge carriers [6].

The processes of light absorption and sunlight conversion are described below:

(1) Active materials absorb photon energy $h\nu$, and the photons energy can help electrons to travel to the lowest unoccupied molecular orbital (LUMO), leaving holes at the highest unoccupied molecular orbital (HOMO). At the same time, an electron and a hole are still bound as an exciton by coulomb attraction forces. (2) The bound exciton

diffuses to the interface between donor phase and acceptor phase. (3) At the interface of donor phase and acceptor phase, exciton sets apart into an electron and a hole. (4) Electron and hole travel separately to cathode and anode. Donor material and acceptor material each has a LUMO level and a HOMO level. The energy difference between the LUMO level of donor and the HOMO level of acceptor has an influence on the open-circuit voltage (V_{oc}). The energy difference of LUMO levels of acceptor material and donor material must be higher than 0.3eV.

The process can be seen below in Figure 2.3

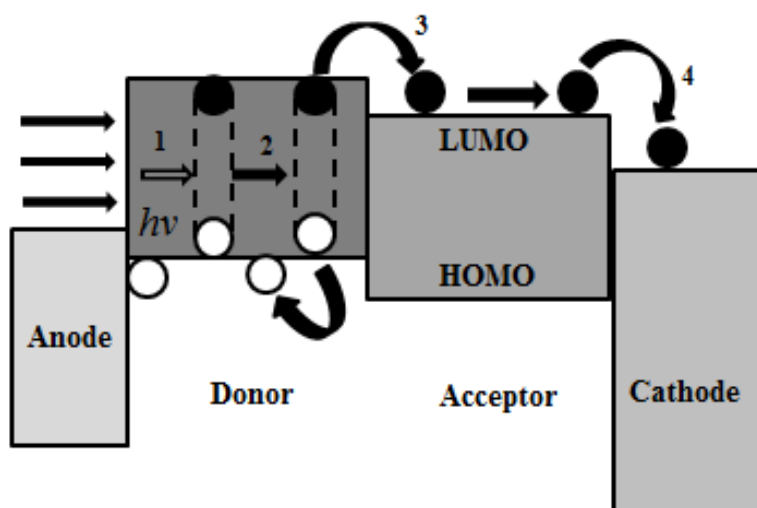


Figure 2.3 Schematic illustration of the photoelectric conversion mechanism [6].

2.1.3 Molecular Orbitals Structures

A carbon atom has $s+p_x+p_y$ atomic orbitals; the $s+p_x+p_y$ atomic orbitals transform into a sp^2 triangular planar and an un-hybridized p_z orbital which is vertical to the sp^2 triangular planar. The sp^2 hybrid orbital forms conventional σ -bond. The σ -bond has fully paired electrons in its bonding state and empty anti-bonding state, resulting in a very strong and stable covalently-bonded molecular backbone. The un-hybridized, half-filled p_z orbital

forms the π -bond [7]. Figure 2.4 (c) and Figure 2.4 (d) show resonant structure and non-resonant structure, respectively.

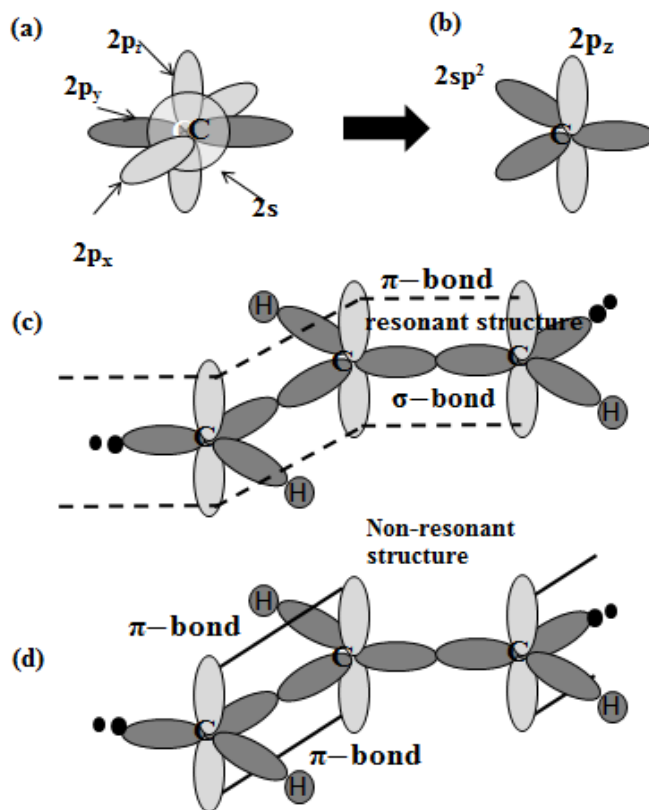


Figure 2.4 A schematic of the hybridization and bonding in chemical structure [7].

2.1.4 Chemical Structures of Conjugated Polymers

In organic polymeric solar cells, there are donor organic materials and acceptor organic materials. Donor organic materials are usually conjugated structure polymers; acceptor organic materials are usually fullerene structure polymers. Delocalized π -electrons are along conjugated backbones of conducting polymers. In addition, formation of delocalized π -electrons is usually through overlap of π -orbital; they can build up a π -system with a filled valence band. In conjugated polymer system, p-type doping assists to remove electrons from the π -system; similarly, n-type doping adds electrons into the π -system; then a charge unit is formed.

Figure 2.5, below, shows the chemical structures of common conjugated polymers.

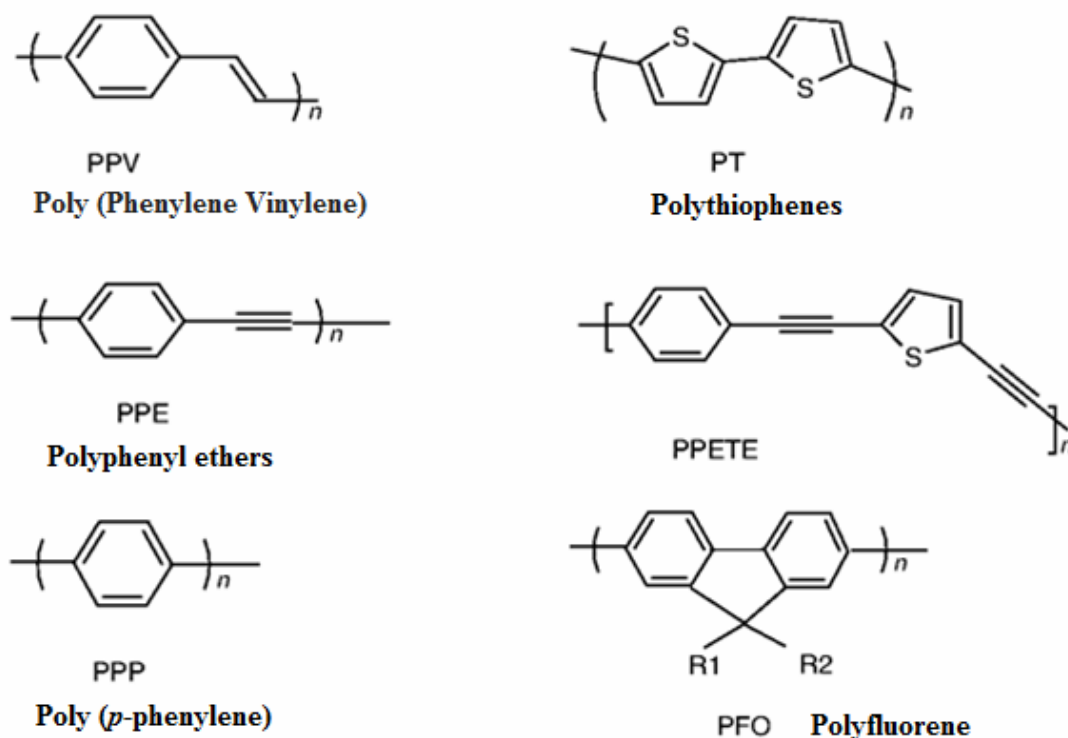


Figure 2.5 Chemical structures of conjugated polymers used in OPVs [8].

2.2 Device Architecture

2.2.1 Typical Device Architecture

In polymeric solar cells, exciton is formed in either donor phase or acceptor phase, and then it will travel to the interface within its lifetime. By this means, the thickness of material must be less than the exciton diffusion length which is 10-20 nm. Within this layer thickness, more light photons can be absorbed. In order to address this requirement, polymeric solar cells need a nano-scale interpenetration network of donor phase material and acceptor phase material [9]. Consequently, efficient dissociation of excitons can be

ensured by transporting charges to the electrodes from the entire photoactive layer within the lifetime of exciton. It is called bulk hetero-junction (BHJ) solar cells [9]. Electron affinity of donor phase and acceptor phase blended polymer is larger than the electron affinity of non-blended polymer. Electron affinity can maintain the stability of exciton. In order to achieve higher power conversion efficiency (PCE), substrate structure should be taken into account. Substrate structure has normal geometry which means front-side illumination, or inverted geometry which means back-side illumination. It depends on whether the front electrode is anode (normal geometry) or cathode (inverted geometry). The metal electrode has to have an appropriate work function, which is a high work function for holes and low work function for electrons [10]. Figure 2.6 shows a simple device structure of polymer solar cell; the organic layer which is used as the active layer usually comprises multiple layers.

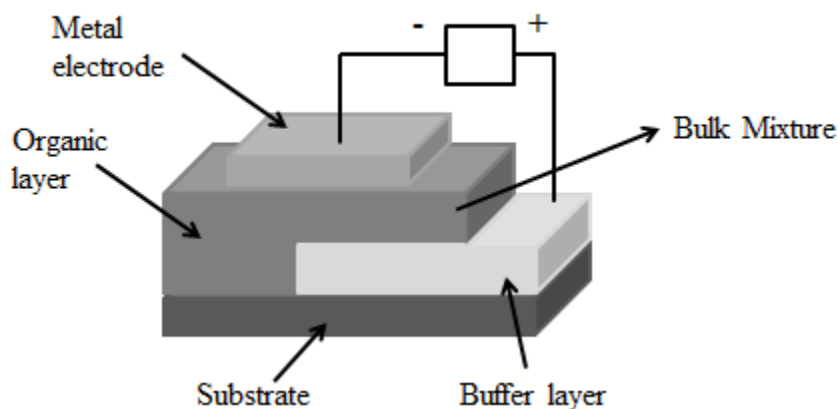


Figure 2.6 Polymeric solar cell device structure.

2.3 Tandem Polymeric Solar Cells

2.3.1 The Need for Tandem Polymeric Solar Cells

Tandem polymeric solar cells are multilayer solar cells. Due to the tandem structure, polymeric solar cells have two or more photovoltaic cells in series; thus, the open circuit voltage, V_{oc} , of cells can be increased. When two cells are connected in series, V_{oc} of tandem solar cells is the sum of V_{oc} of sub-cells, $V_{oc1} + V_{oc2} = V_{oc (tandem)}$ [11]. Commonly, multilayer cells use different band-gap materials, one is a larger band-gap semiconductor and the other is a smaller band-gap semiconductor [12]. Consequently, the light harvesting will be improved. PCE of tandem polymeric solar cells is better than PCE of single cell made with the same material. Larger band-gap semiconductor and smaller band-gap semiconductor together can excite more excitons. Figure 2.7 shows a typical structure of tandem polymeric solar cells.

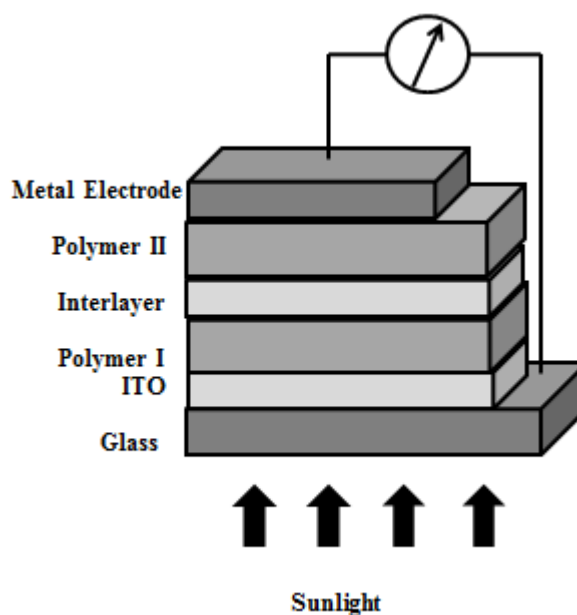


Figure 2.7 Typical tandem polymeric solar cell device.

2.3.2 Fabrication of Tandem Polymeric Solar Cells

The process of fabricating active layers has three categories: all vacuum processing, all solution processing and a combination of vacuum and solution. Stacked polymeric solar cells cannot be fabricated by solution process easily. Difficulties of depositing sequential layers can almost be solved by vacuum processing of small molecules [13-16]. Since a first layer can be solution processed and the second layer vacuum deposited, this approach conceptually follows suite along with all solution processed devices employing orthogonal solvents and carefully chosen interfacial layers [17-19]. This approach has led to the highest reported efficiency of 6.5% for a polymeric solar cell [19].

A novel concept was developed whereby the tandem solar cell is realized in a reflective geometry thus avoiding complex multilayer solution processing [20]. One of the strengths of polymer and organic solar cells is the possibility for all solution processing and, while this has been demonstrated for tandem cells with evaporated metal electrodes, there are still severe limitations to the choice of solvents and the order of application of the individual layers [21].

The approach has so far employed different solvents for the different layers that are orthogonal. The next solvent in the process is a poor one for the material in the previously deposited layer [21]. When the first layer is formed and a dry thin film is made, it is difficult to process the next layer from solution because of the solvent occupied which may dissolve the first layer totally or partially. From this point of view, solubility properties of various layers can be controlled as stated by selecting appropriate solvents. Tandem polymeric solar cells have at least 6 layers or more; it is not practical to switch so many different solvents.

A new approach is that materials can be processed from solution and then made insoluble by a thermal treatment. Labile bond of the molecule, which is the linker to the solubility group, has the active material as its backbone. For example, the soluble group is a branched alkyl chain attached to the active conjugated polymer backbone through an ester bond. The bond breaks when it is heated eliminating a volatile alkene and leaving the polymer component insoluble [21].

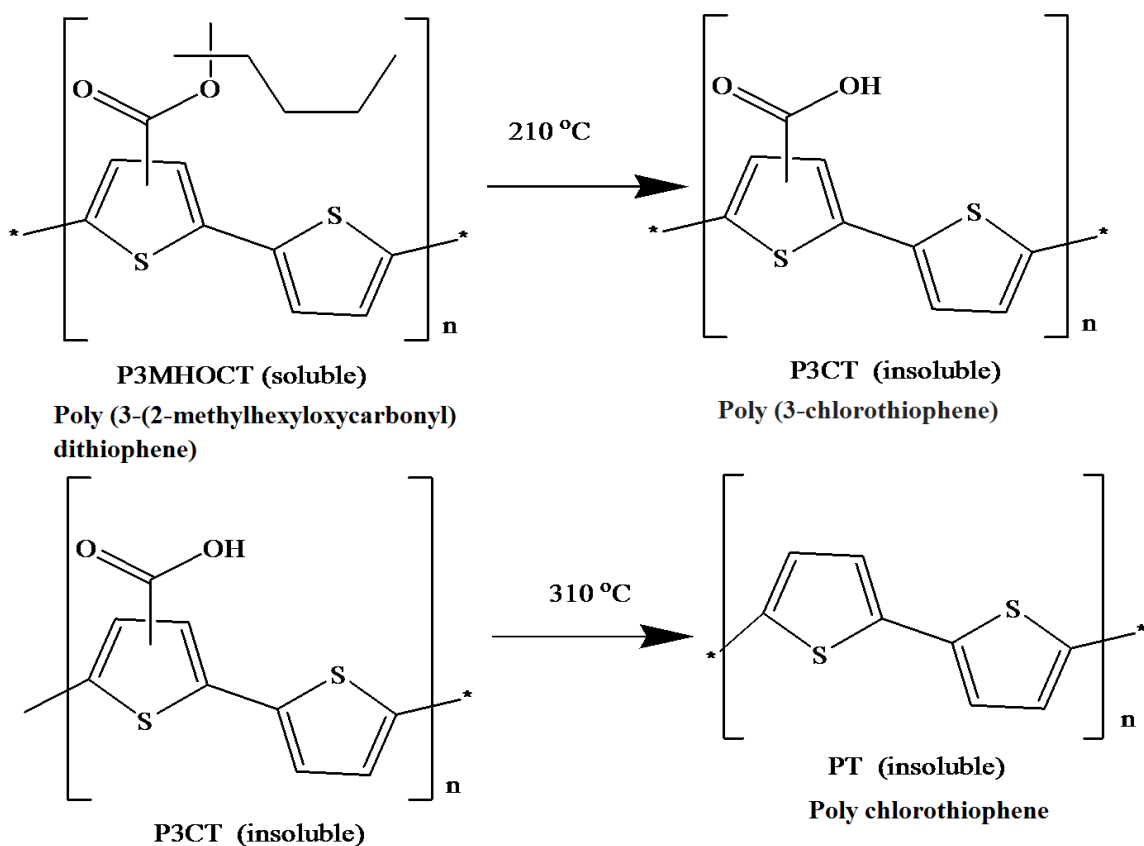


Figure 2.8 Thermo-treatment process.

By this way, when subsequent layers are processed, there is no limit to the choice of the solvent. Sequential layers can be deposited from any solvent including the possibility of using the same solvent throughout the process [21]. There is no limit to the choice of processing solvent in the whole process. After thermal treatment, the material is

called thermo-cleavable. An all solution processed tandem polymer solar cells based on thermo-cleavable materials has been reported by Hagemann et al. [22].

CHAPTER 3

RESEARCH OBJECTIVE

Poly (3-hexylthiophene): [6, 6]-phenyl C₆₁-butyric acid methylester (P3HT: PCBM) and poly[2,1,3-benzothiadiazole-4,7-diyl[4,4-bis(2-ethylhexyl)-4H-cyclopenta[2,1-b:3,4-b']dithiophene-2,6-diyl]]: [6, 6]-phenyl C₆₁-butyric acid methylester (PCPDTBT: PCBM) are used as active layer materials in polymeric solar cells. Analysis of Microelectronic and Photonic Structures - One Dimension (AMPS-1D), which has been developed by Pennsylvania State University, is utilized to the simulate current-voltage (I-V) characteristics of single polymeric solar cells and tandem polymeric solar cells. Additional comparison of the current-voltage (I-V) characteristics of poly (3, 4-ethylenedioxythiophene): poly (styrenesulfonate) (PEDOT: PSS) and indium oxide (In₂O₃) and tin oxide (SnO₂) (ITO) as transparent layer materials are simulated by Analysis of Microelectronic and Photonic Structures One Dimensional (AMPS-1D).

CHAPTER 4

EXPERIMENTAL DETAILS

4.1 AMPS-1D

AMPS-1D stands for Analysis of Microelectronic and Photonic Structures - One Dimension. It was engineered to be a very general and versatile computer simulation tool for the analysis of device physics and device design. It is a one-dimensional (1-D) device physics code which is applicable to any two terminal device. It can be used for diode, sensor, photodiode, and photovoltaic device analysis [23].

AMPS-1D is the creation of Professor Stephen Fonash and his team of students and visiting scholars: John Arch, Joe Cuiffi, Jingya Hou, William Howland, Peter McElheny, Anthony Moquin, Michael Rogosky, Francisco Rubinelli, Thi Tran and Hong Zhu [23].

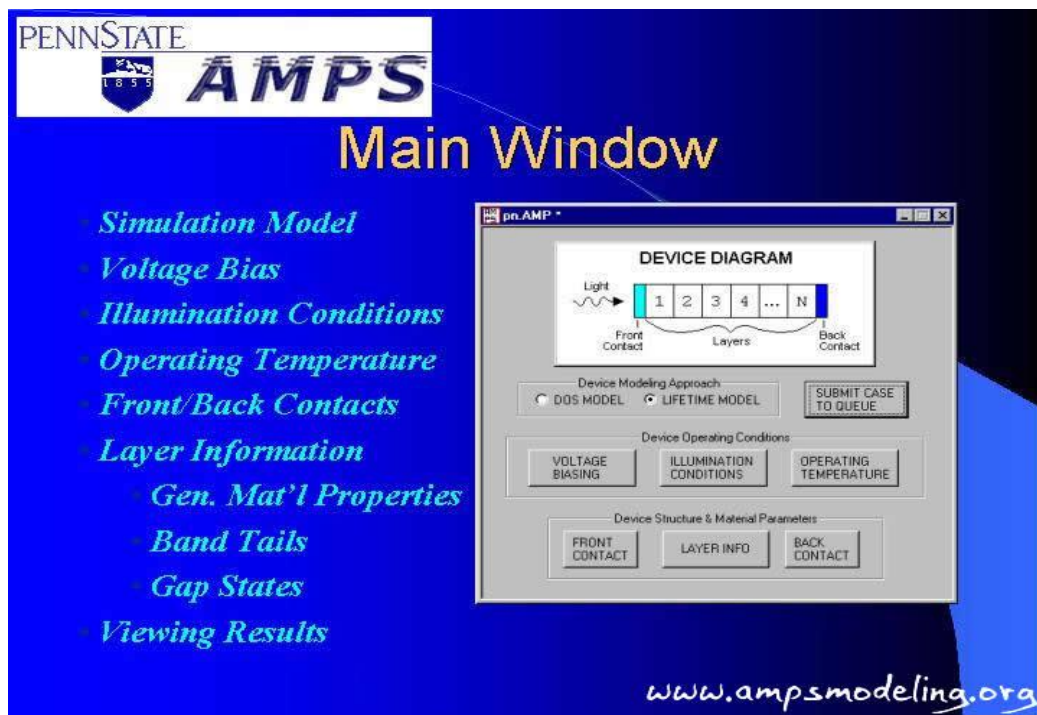


Figure 4.1 AMPS-1D main window [23].

The key part of AMPS-1D is to solve two continuity equations and Poisson's equation with six boundary conditions. All parameters needed are fit to these three equations and then all related values are calculated.

4.2 Molecular Structures of Materials of Polymeric Solar Cells

[6, 6]-phenyl C₆₁-butyric acid methylester (PCBM) is a fullerene derivative of the C₆₀ buck-ball. It is an electron acceptor material which is a more widely used material in polymeric solar cells than fullerenes, due to its solubility in chlorobenzene.

Poly (3-hexylthiophene) (P3HT) comes from the polymerization of thiophenes. P3HT can become conducting when electrons are added or removed from the conjugated π -orbital via doping [24].

Poly (3, 4-ethylenedioxythiophene) poly (styrenesulfonate) (PEDOT: PSS) is a conducting polymer based on 3, 4-ethylenedioxythiophene or PEDOT monomer. Advantages of this polymer are optical transparency in its conducting state, high stability, moderate band gap and low redox potential. A large disadvantage is its poor solubility which is partly circumvented in the PEDOT composite [25].

ITO is a solid solution of indium (III) oxide (In₂O₃) and tin (IV) oxide (SnO₂), typically 90% In₂O₃, 10% SnO₂ by weight. In the infrared region of the spectrum, it acts as a metal-like mirror.

Poly[2,1,3-benzothiadiazole-4,7-diyl[4,4-bis(2-ethylhexyl)-4H-cyclopenta[2,1-b:3,4-b']dithiophene-2,6-diyl]] (PCPDTBT) is a kind of popular conjugated material.

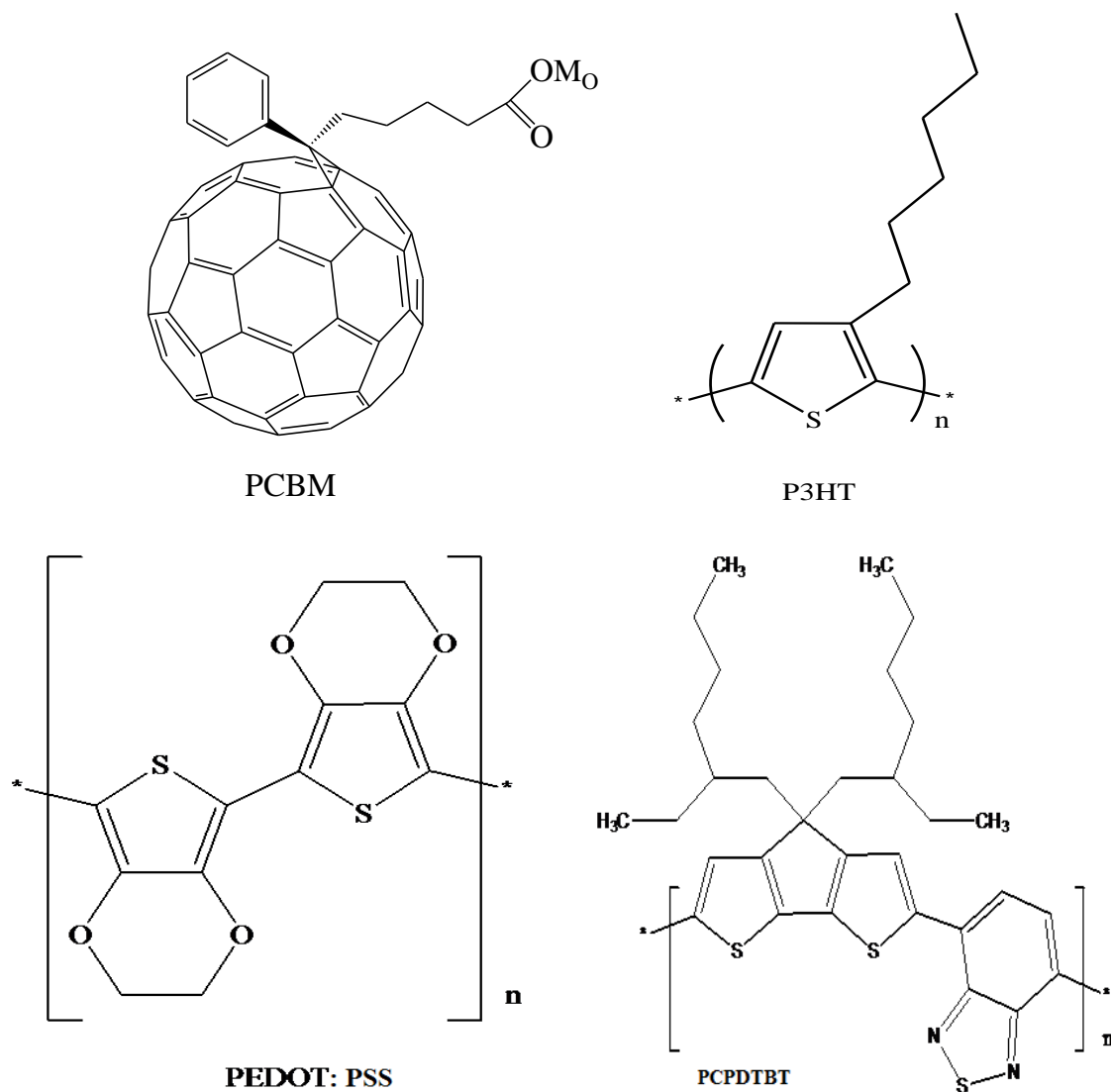


Figure 4.2 Molecular structures: PCBM, P3HT, PEDOT: PSS, PCPDTBT.

4.3 Experimental Parameters and Design

4.3.1 Parameters of Polymeric Solar Cell Materials

- i. Front contact, back contact, Fermi level position and Bulk recombination

parameters are described below.

SNO/SNL: Electron recombination speed

SPO/SPL: Hole recombination speed

RF/RB: Reflection coefficient

PHIBO/PHIBL: Barrier height

ND: State density for the donor Gaussian
 GSIG/ND: Capture cross section of the donor-like Gaussian state for electrons
 GSIG/PD: Capture cross section of the donor-like Gaussian state for holes

Table 4.1 General Experimental Data

Front contact SNO=SPO=1e+7 cm/s PHIBO=work function-LUMO (donor)	Back contact SNL=SPL=1e+7 cm/s PHIBL=work function-LUMO (acceptor)
Bulk Recombination Donor Like: ND=1e+10 #/cm ³ GSIG/ND=1e-9 cm ² GSIG/PD=1e-10 cm ²	Bulk Recombination Acceptor Like: ND=1e+10 #/cm ³ GSIG/ND=1e-10 cm ² GSIG/PD=1e-9 cm ²

ii. Important general layer parameters and their explanations are described below.

EPS: Dielectric constant
 MUN: Electron mobility
 MUP: Hole mobility
 NC: Conduction band effective density of state
 NV: Valence band effective density of state
 NA: Number of acceptors
 ND: Number of donors
 EG: Energy of band-gap
 CHI: Electron affinity

Tables 4.2-4.6 show general layer parameters of employed materials needed for AMPS-1D simulations.

Table 4.2 PEDOT: PSS General Layer Data

Parameter	EPS	MUN	MUP	NC	NV
Value	3.0	1.0e-4	1.0e-3	1.0e+22	1.0e+22
Unit		cm ² /V/S	cm ² /V/S	cm ³	cm ³
Parameter	NA	ND	EG	CHI	
Value	0.0	0.0	1.6	3.4	
Unit	#/cm ³	#/cm ³	eV	eV	

Table 4.3 PCBM General Layer Data

Parameter	EPS	MUN	MUP	NC	NV
Value	3.0	1.0e-3	1.0e-4	1.0e+22	1.0e+22
Unit		cm ² /V/S	cm ² /V/S	cm ³	cm ³
Parameter	NA	ND	EG	CHI	
Value	3.17e+13		2.1	3.70	
Unit	#/cm ³	#/cm ³	eV	eV	

Table 4.4 P3HT General Layer Data

Parameter	EPS	MUN	MUP	NC	NV
Value	3.4	1.0e-4	1.0e-3	1.0e+22	1.0e+22
Unit		cm ² /V/S	cm ² /V/S	cm ³	cm ³
Parameter	NA	ND	EG	CHI	
Value	3.17e+13		1.85	3.10	
Unit	#/cm ³	#/cm ³	eV	eV	

Table 4.5 PCPDTBT General Layer Data

Parameter	EPS	MUN	MUP	NC	NV
Value	3.4	3.5e-4	1.5e-3	1.0e+22	1.0e+22
Unit		cm ² /V/S	cm ² /V/S	cm ³	cm ³
Parameter	NA	ND	EG	CHI	
Value	4.0e+13		1.5	3.7	
Unit	#/cm ³	#/cm ³	eV	eV	

Table 4.6 ITO General Layer Data

Parameter	EPS	MUN	MUP	NC	NV
Value	4.6	210		4.1e+18	
Unit		cm ² /V/S	cm ² /V/S	cm ³	cm ³
Parameter	NA	ND	EG	CHI	
Value			2.75 (indir) 3.6-3.75 (dir)	4.1	
Unit	#/cm ³	#/cm ³	eV	eV	

- i. Important band tail parameters and their explanations are described below.

ED: Energy E_d for donor-like tails
GDO: $g_d = GDO \exp(E/E_d - E_v/E_d)$
TSIG/ND: Electrons in donor tail states
TSIG/PD: Holes in donor tail states
EA: Energy E_a for acceptor-like tails
GAO: $g_a = GAO \exp(E/E_d - E_v/E_d)$
TSIG/NA: Electrons in acceptor tail states
TSIG/PA: Holes in acceptor tail states

Tables 4.7- 4.9 show band tail parameters of employed materials needed for AMPS-1D simulations [23].

Table 4.7 PEDOT: PSS Band Tail Data

Parameter	ED	GDO	TSIG/ND	TSIG/PD	EA
Value	1.05	1.0e+10	1.0e-9	1.0e-10	1.05
Unit	eV	$\#/cm^3/eV$	cm^2	cm^2	eV
Parameter	GAO	TSIG/NA	TSIG/PA		
Value	1.0e+10	1.0e-10	1.0e-9		
Unit	$\#/cm^3/eV$	cm^2	cm^2		

Table 4.8 P3HT Band Tail Data

Parameter	ED	GDO	TSIG/ND	TSIG/PD	EA
Value	1.05	1.0e+10	1.0e-9	1.0e-10	1.05
Unit	eV	$\#/cm^3/eV$	cm^2	cm^2	eV
Parameter	GAO	TSIG/NA	TSIG/PA		
Value	1.0e+10	1.0e-10	1.0e-9		
Unit	$\#/cm^3/eV$	cm^2	cm^2		

Table 4.9 PCBM Band Tail Data

Parameter	ED	GDO	TSIG/ND	TSIG/PD	EA
Value	1.05	1.0e+10	1.0e-9	1.0e-10	1.05
Unit	eV	#/cm ³ /eV	cm ²	cm ²	eV
Parameter	GAO	TSIG/NA	TSIG/PA		
Value	1.0e+10	1.0e-10	1.0e-9		
Unit	#/cm ³ /eV	cm ²	cm ²		

ii. Absorption coefficient parameters

Absorption coefficient determines how far light can penetrate into materials at a particular wavelength before it is absorbed. The absorption coefficient depends on the optical characteristics of the material and the wavelength of light. Semiconductor materials have a sharp edge in their absorption coefficient since photons with energy lower than the band gap energy cannot excite an electron into the conduction band from the valence band.

4.3.2 Design of Comparable Experiments

The active layer of bulk-hetero-junction (BHJ) solar cells is a mixture of nano-scale donor materials and nano-scale acceptor materials. Exciton is created inside the BHJ and then it can diffuse to the interface to form donor and acceptor within its diffusion length. Obviously, active layer structure of simulation device can be designed as a donor layer, a generation layer and an acceptor layer.

PEDOT: PSS has similar EQE as ITO and its conductivity is high enough to be used as the electrode for the diode. These two organic solar cells are under high-intensity illumination of AM 1.5 ($1000\text{W}/\text{m}^2$)

Part I of simulations by AMPS-1D: (1) PEDOT: PSS transport layer polymeric solar cell. (2) ITO transport layer polymeric solar cell. Figure 4.3 shows device structures of these two organic solar cells:

Table 4.9 Thickness of Polymeric Solar Cells Layers

	Generation	ITO	P3HT:PCBM	PEDOT: PSS
Thickness (nm)	2	2	100	2

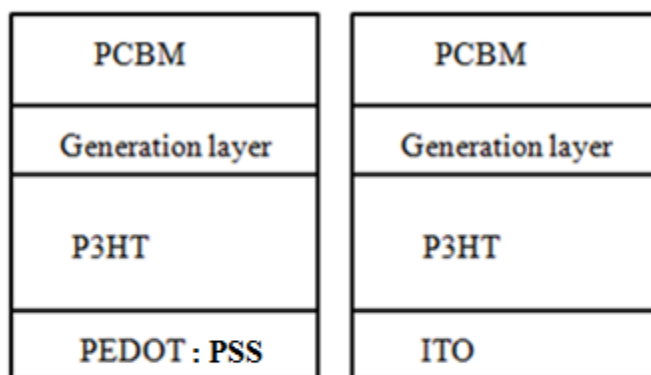
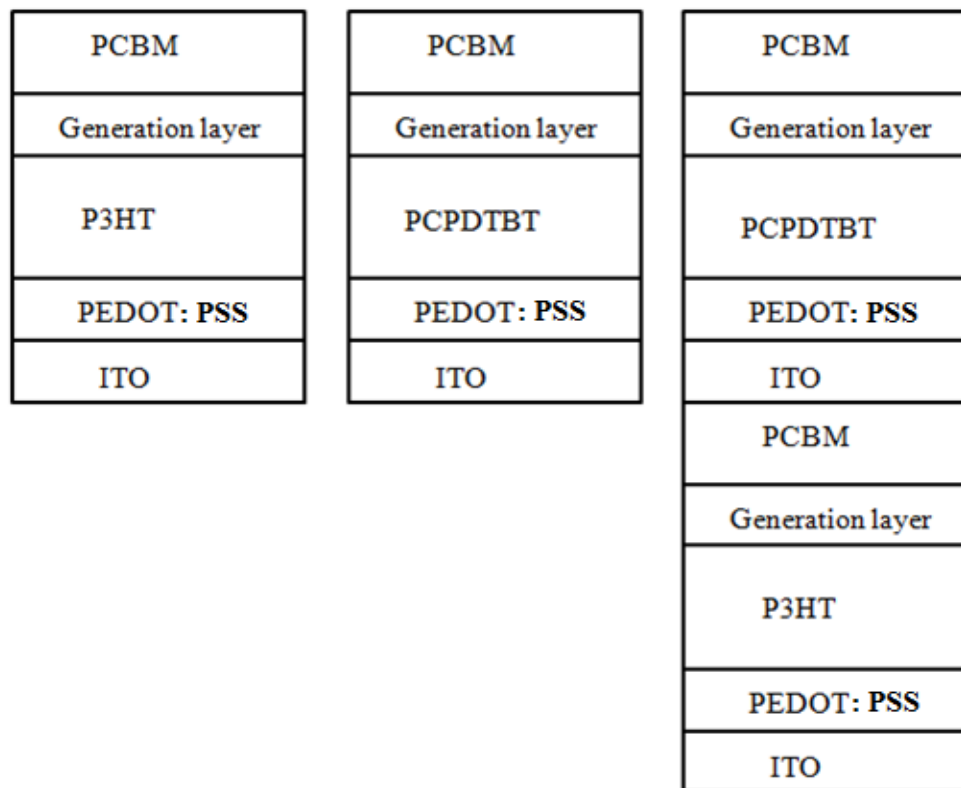


Figure 4.3 Device structures of organic solar cells.

Part II of simulations by AMPS-1D is to compare the PCE of single polymeric solar cells with PCE of tandem polymeric solar cells. Figure 4.4 shows the proposed device structures.

Table 4.10 Thickness of Polymeric Solar Cells Layers

	Generation	ITO	PEDOT: PSS	PCBM	P3HT	PCPDTBT
Thickness (nm)	2	2	2	50	50	50

**Figure 4.4** Device structures of single polymeric solar cells and tandem polymeric solar cells.

CHAPTER 5

RESULTS, DISCUSSION AND CONCLUSIONS

Comparison of the results of Part I and Part II are obtained by building suitable parameters of organic polymers for AMPS-1D.

- a) Figure 5.1 shows the current-voltage (I-V) curves between PEDOT: PSS transport layer polymeric solar cell and ITO transport layer polymeric solar cell.

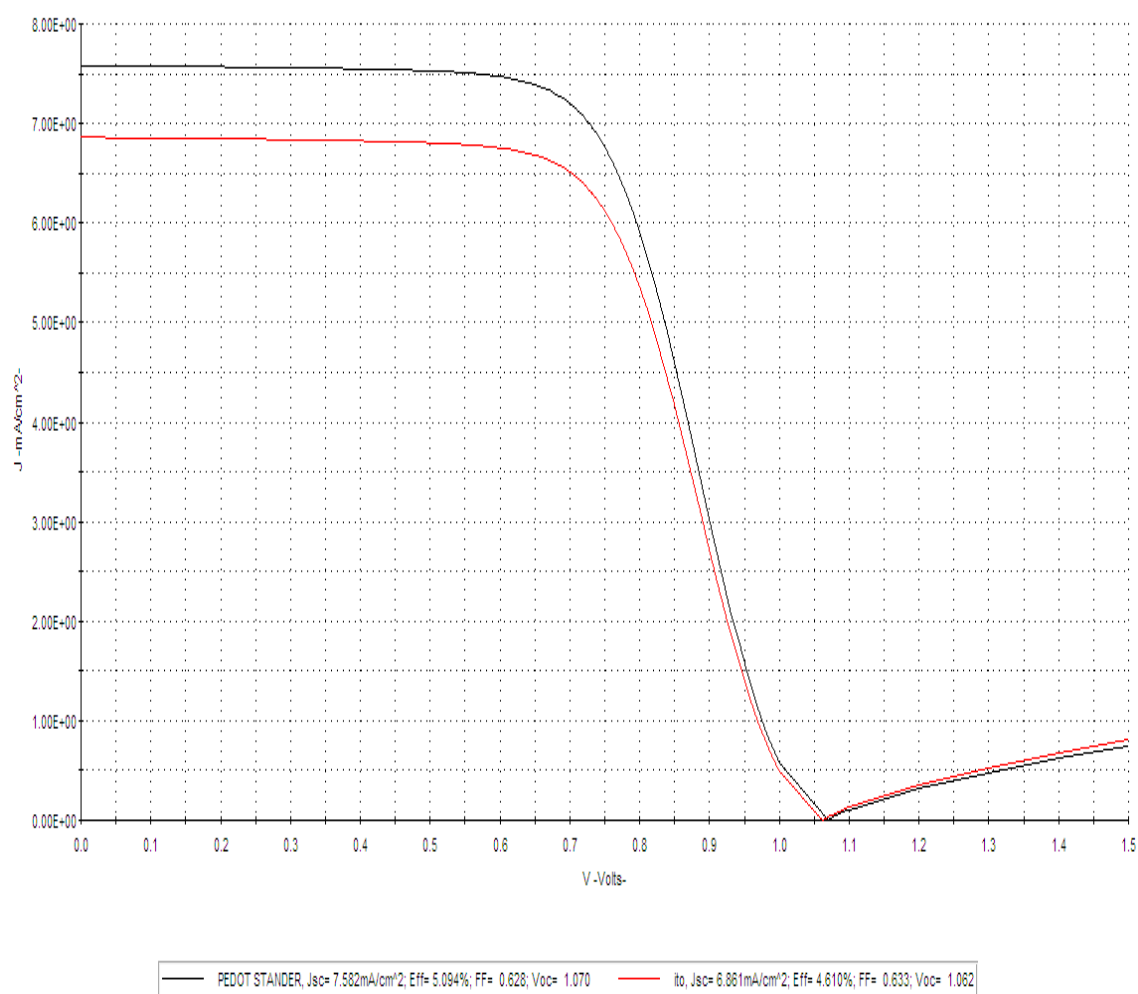


Figure 5.1 I-V curves: PEDOT: PSS transport layer polymeric solar cell and ITO transport layer polymeric solar cell.

Table 5.1 Characteristics of PEDOT: PSS Transport Layer Polymeric Solar Cell and ITO Transport Layer Polymeric Solar Cell

Anode	J_{SC} (mA/cm^2)	V_{oc} (V)	FF	PCE (%)
PEDOT: PSS	7.582	1.070	0.628	5.094
ITO	6.861	1.062	0.633	4.61

From Table 5.1, power conversion efficiency of PEDOT: PSS is higher than that of ITO. PEDOT: PSS is transparent and has good conductivity. The reason for higher efficiency is that the work function of PEDOT: PSS is closer to the first layer in the conduction band.

b) Single polymeric solar cells versus Tandem polymeric solar cells.

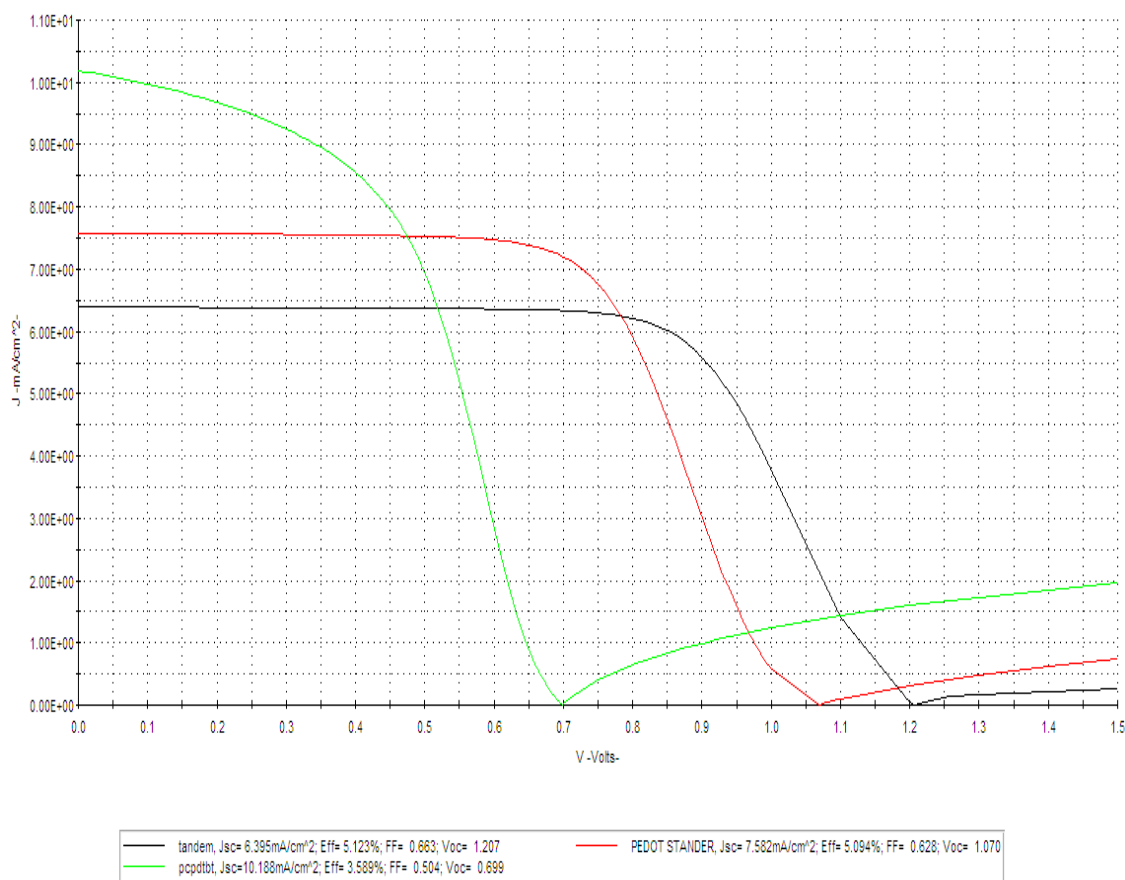


Figure 5.2 I-V curves: Single polymeric solar cells and tandem polymeric solar cells.

Table 5.2 Characteristics of Single Polymeric Solar Cells and Tandem Polymeric Solar Cells

<i>Anode</i>	J_{SC} (mA/cm^2)	V_{OC} (V)	<i>FF</i>	<i>ECE</i> (%)
PCPDTBT: PCBM	10.188	0.699	0.504	3.589
P3HT: PCBM	7.582	1.070	0.628	5.094
Tandem	6.395	1.207	0.663	5.123

In AMPS-1D, transport layers are considered as front and back contact conditions. Simulation with middle transport layer was not successful. This is because the middle transport layer is considered as black and blocks the sunlight through the entire solar cell. In the simulations of tandem solar cells, there is no transport layer between two single solar cells.

From the results of the simulations, power conversion efficiency of P3HT: PCBM polymer solar cell is noted to be higher than that of PCPDTBT: PCBM polymer solar cell. The power conversion efficiency of tandem solar cells is 5.123%, which is not consistent with the experimental results that have been reported in the literature. PCE of tandem polymeric solar cells is slightly higher than that of P3HT: PCBM polymeric solar cell. The reason for similar PCEs of tandem solar cells and P3HT: PCBM polymeric solar cell is that the total short-current of tandem solar cells follows the lower one of two single polymeric solar cells.

Interestingly, open circuit voltage is due to the linearity of the donor HOMO level and the acceptor LUMO level. $V_{oc}=1.207$ of tandem polymeric solar cells is not exactly

equal to the sum of V_{oc} of these two single polymeric solar cells. AMPS-1D considers transport layers as front contact and back contact. Tandem polymeric solar cells need a transport layer that is connected to two single polymeric solar cells; the software cannot support suitable parameters for it. In order to fulfill tandem polymeric solar cell simulation by AMPS-1D, the tandem polymeric solar cell design cannot be simply a composition of two or more single polymeric solar cells. Thickness of each single polymeric solar cell must be calculated ahead.

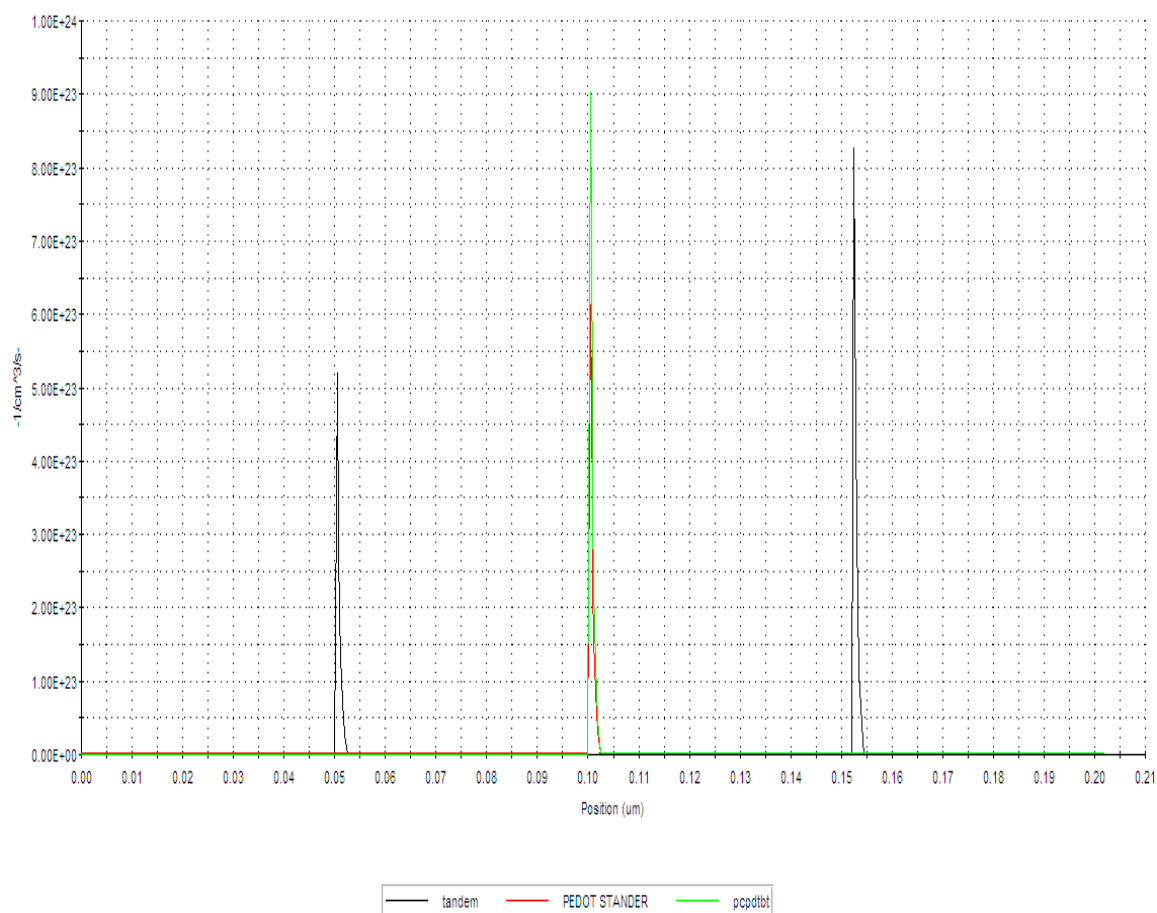


Figure 5.3 Generation positions of single and tandem polymeric solar cells.

From Figure 5.3, the generation positions in tandem polymeric solar cells are in the range of 50-52nm and 152-154nm. The generation positions of single polymeric solar

cells are both in the 110-112nm range. All generation positions range with the thickness of polymeric solar cells.

c) Incident photon current efficiency (IPCE)

IPCE can be calculated by equation 5.1

$$\text{IPCE} = 1240 * I_{sc} / \lambda * P_{in} \quad (5.1)$$

For $\lambda = 600 \text{ nm}$

P3HT: PCBM polymer solar cells, $\text{IPCE} = 1240 * 15.683e-2 / 600e-9 * 1000 = 0.32$

PCPDTBT: PCBM polymer solar cells, $\text{IPCE} = 1240 * 14.326e-2 / 600e-9 * 1000 = 0.296$

Tandem solar cells, $\text{IPCE} = 1240 * 17.321e-2 / 600e-9 * 1000 = 0.358$

A low IQE indicates that the active layer of the solar cell is unable to make good use of the photons.

REFERENCES

1. www.applied-solar.info/solar-energy/history-of-solar-cells, accessed date 03/05/2012.
2. Perlin, J. *From Space to Earth: The Story of Solar Electricity*. Cambridge, MA: Harvard University Press, 2002.
3. www.californiasolarcenter.org/history.html, accessed date 03/15/2012.
4. Fan, L. J., and Wayne E. Jones Jr. *Energy Transfer and Electronic Energy Migration Process*. Hoboken, New Jersey: A John Wiley & Sons, Inc., Publication, 2010.
5. Lane, P. A., and Z. H. Kafafi. *Solid-State Organic Photovoltaics: A Review of Molecular and Polymeric Devices*. Boca Raton, FL: Taylor & Francis Group, LLC, 2005.
6. Gregg, B. A., and M. C. Hanna. "Comparing organic to inorganic photovoltaic cells: Theory, Experiment and Simulation." *Applied Physics Letters* 93 (2003): 3605-3614.
7. Rockett, Angus. *The Materials Science of Semiconductors*. New York, NY: Springer Science +Business Media, LLC, 2007.
8. Allen, Norman S. *Photochemistry and Photophysics of Polymer Materials*. Hoboken, New Jersey: John Wiley & Sons, Inc., Publication, 2008.
9. Wang, W., E.A. Schiff and Q. Wang. "Amorphous Silicon Polyaniline Heterojunction Solar Cells: Fermi Levels and Open Circuit Voltages." *Journal of Non-Crystalline Solids* 354 (2008): 2862-65.
10. Krebs, F. C. *Polymeric Solar Cells Materials, Design, Manufacture*, Lancaster, Pennsylvania: DEStech Publication, 2010.
11. Helgesen, M., R. Søndergaard, and F. C. Krebs. "Advanced Materials and Processes for Polymer Solar Cell Devices." *Journal of Materials Chemistry* 20 (2010): 36-60.
12. Wanlass, M. W., "Practical Considerations in Tandem Cell Modeling." *Solar Cells* 27, no. 1-4 (1989): 191-204.
13. A. Yakimov, and S.R. Forrest. "High Photovoltage Multiple-Heterojunction Organic Solar Cells Incorporating Interfacial Metallic Nanoclusters." *Applied Physics Letters* 80, no.9 (2002).

14. Xue, J., S. Uchida, B.P. Rand, and S.R. Forrest. "Asymmetric Tandem Organic Photovoltaic Cells with Hybrid Planar-Mixed Molecular Heterojunctions." *Applied Physics Letters* 85, no. 23 (2004): 5757-5759.
15. Xue, J., S. Uchida, B.P. Rand, and S.R. Forrest. "4.2% Efficient Organic Photovoltaic Cells with Low Series Resistance." *Applied Physics Letters* 84, no. 16 (2004).
16. Cheyng, D., H. Gommans, M. Odijk, J. Poortmans, and P. Heremans. "Stacked Organicsolar Cells based on Pentacene and C₆₀." *Solar Energy Materials and Solar Cells* 91, no. 5 (2007): 399-404.
17. Colsmann, A., J. Junge, C. Kayser, and U. Lemmer. "Organic Tandem Solar Cells Comprising Polymer and Small-Molecule Subcells." *Applied Physics Letters* 89, no. 20 (2006).
18. Gilot, J., M.M. Wienk, and R.A.J. Janssen. "Double and Triple Junction Polymeric Solar Cell Processed from Solution." *Applied Physics Letters* 90 no. 14 (2007).
19. Kim, J.Y., K. Lee, N.E. Coates, D. Moses, T.-Q. Nguyen, M. Dante, and A.J. Heeger. "Efficient Tandem Polymeric Solar Cells Fabricated by All-Solution Processing." *Science*, 2007, 222-25.
20. Tvingstedt, K., V. Andersson, F. Zhang, and O. Inganäs. "Folded Reflective Tandem Polymer Solar Cell Doubles Efficiency." *Applied Physics Letters* 91, no. 12 (2007).
21. Hagemann, O., M. Bjerring, N. C. Nielsen and F. C. Krebs. "All Solution Processed Tandem Polymeric Solar Cells Based on Thermo-cleavable Materials." *Solar Energy Materials & Solar Cells* 92 no. 11 (2008): 1327-1335.
22. www.ampsmodeling.org/default.html, accessed date 04/05/2012.
23. en.wikipedia.org/wiki/P3HT, accessed date 04/05/2012.
24. en.wikipedia.org/wiki/PEDOT, accessed date 04/05/2012.